

# Transition from transient to stationary behavior in stimulated Raman scattering

F. Sanborn and C. R. Menyuk

Department of Computer Science and Electrical Engineering, University of Maryland, Baltimore County, Baltimore, Maryland 21228-5398

Received 14 March 1996

The transition between the transient and the stationary regimes of stimulated Raman scattering is examined computationally for pulses with a sharp initial rise. We find that the transient-regime predictions are useful for times less than  $T_2$  regardless of the pulse duration and that the stationary-regime predictions become useful only for times much greater than  $T_2$ . © 1996 Optical Society of America.

Fundamental studies of stimulated Raman scattering in molecular gases are often carried out in  $H_2$  and  $D_2$  because the scattering is strong and the behavior is relatively simple in these gases.<sup>1</sup> Typically, collimated beams of pump and Stokes radiation are injected into a Raman cell that is roughly a meter long, while pulse durations vary from 40 ps to 100 ns.<sup>2-5</sup> Long-focal-length beams are used to minimize the importance of transverse effects, which can then be either ignored or taken into account by a simple transformation of the axial coordinate. The Stokes radiation is generated in a separate cell by spontaneous emission. Multipass cells are sometimes used to increase the interaction length and to suppress the generation of higher-order Stokes radiation.<sup>4</sup> Under these circumstances, Wang<sup>6</sup> showed many years ago that the basic equations that govern the evolution of the pump and the Stokes waves in the Raman cell may be written

$$\frac{1}{c} \frac{\partial E_1}{\partial t} + \frac{\partial E_1}{\partial x} = -i \frac{k_1}{k_2} \kappa_2 E_2 Q, \quad (1a)$$

$$\frac{1}{c} \frac{\partial E_2}{\partial t} + \frac{\partial E_2}{\partial x} = -i \kappa_2 E_1 Q^*, \quad (1b)$$

$$\frac{\partial Q}{\partial t} + \frac{1}{T_2} Q = -i \kappa_1 E_1 E_2^*, \quad (1c)$$

where  $x$  and  $t$  are the distance along the Raman cell and time,  $E_1$  and  $E_2$  are the complex envelopes of the pump and the Stokes fields,  $Q$  is the complex envelope of the material excitation that corresponds to the off-diagonal element of the density matrix,  $k_1$  and  $k_2$  are the wave numbers of the pump and the Stokes fields,  $\kappa_1$  and  $\kappa_2$  are the standard Raman coefficients first introduced by Wang,<sup>6</sup> and  $T_2$  is the collisional de-excitation time.

It is useful to use retarded time, i.e., to make the transformation  $x' = x$ ,  $t' = t - x/c$ , which eliminates the  $t$  derivatives from Eqs. (1a) and (1b). It is also useful to normalize Eqs. (1) so that the parameters  $\kappa_1$  and  $\kappa_2$  do not appear. There is no unique way to do this, but one way that is physically meaningful is to set

$$\chi = x'/L, \quad \tau = t'/T_{\text{pulse}}, \quad \gamma = T_{\text{pulse}}/T_2,$$

$$A_1 = \frac{E_1}{E_{\text{max}}}, \quad A_2 = \left(\frac{k_1}{k_2}\right)^{1/2} \frac{E_2}{E_{\text{max}}},$$

$$X = i \left(\frac{k_1}{k_2}\right)^{1/2} \frac{Q}{\kappa_1 E_{\text{max}}^2 T_{\text{pulse}}}, \quad (2)$$

where  $T_{\text{pulse}}$  is the duration of the pump pulse and  $E_{\text{max}}$  is the maximum value of the pump field. The characteristic length scale  $L$  is then fixed, and one finds  $L = 1/\kappa_1 \kappa_2 E_{\text{max}}^2 T_{\text{pulse}}$ , so that  $L$  is inversely proportional to the initial energy of the injected pump pulse if the pulse shape is fixed. We thus obtain the normalized equations

$$\frac{\partial A_1}{\partial \chi} = -A_2 X, \quad (3a)$$

$$\frac{\partial A_2}{\partial \chi} = A_1 X^*, \quad (3b)$$

$$\frac{\partial X}{\partial \tau} + \gamma X = A_1 A_2^*. \quad (3c)$$

In the experiments to date,  $T_2$  varies within the range 600 ps–1.2 ns, depending on the gas pressure, which is just a factor of 2, while the pump duration varies from 40 ps through 100 ns, which is three orders of magnitude.<sup>2-5</sup> Thus for control of the parameter  $\gamma$  that appears in Eqs. (2) and (3) it is most natural to change to pulse duration. One can increase  $\gamma$  without altering the characteristic length scale  $L$  by keeping the pump pulse's energy fixed while increasing its duration. The appropriate boundary conditions are that  $A_1(\chi = 0, \tau) = A_{1,0}(\tau)$  and  $A_2(\chi = 0, \tau) = A_{2,0}(\tau)$  are specified for all  $\tau$ , which implies physically that the time history of the pump and the Stokes radiation is known at the entry to the Raman cell, and  $X(\chi, \tau) \rightarrow 0$  for all  $\chi$  as  $\tau \rightarrow -\infty$ , which implies physically that the material is unexcited before the radiation enters the Raman cell. Mathematically, Eqs. (3) together with these boundary conditions constitute a well-posed boundary-value problem with a unique solution.<sup>7</sup>

There are two limits in which the evolution of the pump and the Stokes radiation is well characterized. The first limit, the so-called stationary limit, occurs when pulse durations are long compared with  $T_2$  and the derivatives of

the pump and the Stokes radiation are initially small compared with  $T_2$ , i.e.,  $|\partial A_{1,0}/\partial\tau| \ll \gamma|A_{1,0}|$  and  $|\partial A_{2,0}/\partial\tau| \ll \gamma|A_{2,0}|$ . In this limit and when  $\tau \gg 1/\gamma$ , the contribution of  $\partial X/\partial\tau$  to Eq. (3c) can be neglected, and this equation becomes  $X = A_1 A_2^*/\gamma$ . Time then appears parametrically in Eq. (3). Noting that  $K^2(\tau) = |A_1(\chi, \tau)|^2 + |A_2(\chi, \tau)|^2$  is constant at each point of  $\tau$  as a function of  $\chi$ , Eqs. (3) can be integrated to yield

$$\begin{aligned} A_1 &= A_{1,0}(\tau) \\ &\times \frac{K(\tau)\exp[-K^2(\tau)\chi/\gamma]}{\{|A_{1,0}(\tau)|^2\exp[-2K^2(\tau)\chi/\gamma] + |A_{2,0}(\tau)|^2\}^{1/2}}, \\ A_2 &= A_{2,0}(\tau) \\ &\times \frac{K(\tau)}{\{|A_{1,0}(\tau)|^2\exp[-2K^2(\tau)\chi/\gamma] + |A_{2,0}(\tau)|^2\}^{1/2}}. \end{aligned} \quad (4)$$

The second limit, the so-called transient limit, occurs when  $T_{\text{pulse}} < T_2$ . In this limit the contribution to Eq. (3c) from the term  $\gamma X$  can be neglected. While the resulting equations do not have a simple analytical solution with the physically realistic boundary conditions that we assumed, these equations can be completely analyzed with the inverse scattering method,<sup>8</sup> and it can be shown that the solution always tends toward a self-similar solution depending only on the combination of variables  $\chi \int_{-\infty}^{\tau} K^2(\tau'') d\tau''$ . This solution has been referred to as an accordion because it appears like an accordion being squeezed from the right in numerical solutions and can be expressed analytically in terms of Painlevé transcendent functions.<sup>1,8</sup>

While self-similar oscillations have been observed experimentally by Duncan *et al.*,<sup>3,5</sup> there has yet to be a careful experiment in which accordions are specifically studied and their properties are carefully compared with the theoretical predictions. The reason that no more than three self-similar oscillations were observed by Duncan *et al.* is that they used a single-pass cell. In the transient regime, both the onset of second Stokes radiation and the number of self-similar oscillations are governed by the dimensionless parameter  $\chi$ .<sup>1,8</sup> Duncan *et al.* obtained values of  $\chi$  as large as several hundred by changing the input-pulse energy, but when  $\chi \geq 50$ , they found that second Stokes radiation became important and destroyed the self-similar oscillations. At  $\chi = 50$  the theory predicts only three self-similar oscillations, which is what was observed. In effect, Eq. (3) became invalid in the real experimental setting when  $\chi \geq 50$ . Shortly thereafter, MacPherson *et al.*<sup>4</sup> demonstrated experimentally that it is possible to avoid second Stokes and anti-Stokes generation completely by use of a multipass cell in which the second Stokes and the anti-Stokes radiation is filtered out at each pass, thus allowing Eqs. (3) to remain valid for almost arbitrarily large values of  $\chi$ , the only practical limitation being the number of passes that can actually be made. MacPherson *et al.*<sup>4</sup> used 18 passes and showed that Eqs. (3) remain valid over the entire length, but they could not observe accordions because they used pulse durations of 100 ns, which is much longer than  $T_2$ . From this discussion it should be apparent that there is

no fundamental barrier to observing accordions. It could be done in principle by combining the short-pulse setup that was used by Duncan *et al.*<sup>5</sup> with the multipass geometry developed by MacPherson *et al.*<sup>4</sup> There is considerable interest in doing so because accordions are a universal phenomenon in the same mathematical sense that solitons are and are expected to appear in a wide variety of systems.<sup>1,8</sup>

Recently, Wessel *et al.*<sup>2</sup> pointed out that it is not really necessary to use pulses that are short compared with  $T_2$ . As long as the leading edge of both the pump and the Stokes radiation has a sharp rise time that is short compared with  $T_2$ , the initial portion of the pulse in which the time is less than  $T_2$  will behave just as if it were in the transient regime. To achieve this rapid rise, they proposed to use an electro-optic modulator to truncate the front-end of long-duration pulses. Over a time scale that is long compared with  $T_2$ , the pulse should exhibit the behavior that is expected in the stationary regime; thus it should be possible to observe a transition from the transient regime to the stationary regime in a single pulse! In this paper we examine this transition numerically, using the procedure described in Ref. 9.

In our simulations we used hyperbolic secant pulses as our initial conditions because passively mode-locked, short-pulse lasers typically produce this shape. We truncated the leading edge of the pulse to obtain a rapid rise in accordance with the proposal of Wessel *et al.*<sup>2</sup> Thus our initial conditions have the form

$$\begin{aligned} A_{1,0}(\tau) &= \alpha H(\tau)\text{sech}(\tau), \\ A_{2,0}(\tau) &= \beta H(\tau)\text{sech}(\tau), \end{aligned} \quad (5)$$

where  $H(\tau) = 1$  when  $\tau \geq 0$  and  $H(\tau) = 0$  when  $\tau < 0$  is the usual Heaviside function, and we took  $\alpha = 1.0$  and  $\beta = 0.01$  in all our simulations, corresponding to initial conditions in which the Stokes wave is small compared with the pump wave but nonnegligible.

We examined a series of  $\gamma$  values ranging from  $\gamma = 0.1$  to  $\gamma = 10.0$ , but in this report we present only the results when  $\gamma = 0.1$ ,  $\gamma = 1.0$ , and  $\gamma = 10.0$  since these values are sufficient to give a good indication of the overall behavior. We recall that  $\gamma$  corresponds physically to  $T_{\text{pulse}}/T_2$  and that the easiest way to change  $\gamma$  in an experiment is to change  $T_{\text{pulse}}$ . The limit  $\gamma = 0.1$  is highly transient at all values of  $\tau$ , and we verified that at this value the evolution of both the pump and Stokes waves is visually indistinguishable from the evolution at  $\gamma = 0$  in the figures that we present. By contrast, the behavior at  $\gamma = 10.0$  differs significantly from the transient behavior, and the evolution is described by the stationary equations, Eqs. (4), when  $\tau$  is sufficiently large. Nonetheless, when  $\tau$  is small, accordions are visible even when  $\gamma = 10.0$ . This result is consistent with the observation that, when  $\gamma\tau \lesssim 1$ , the behavior will be transient regardless of the size of  $\gamma$  since the evolution at later times depends on the evolution at earlier times. This fact is exploited by Wessel *et al.*<sup>2</sup> in their proposal to use the beginning of long pulses to explore transient behavior.

Figures 1–3 show successively the evolution at  $\chi = 50$ ,  $\chi = 100$ , and  $\chi = 200$ . We focused on these val-

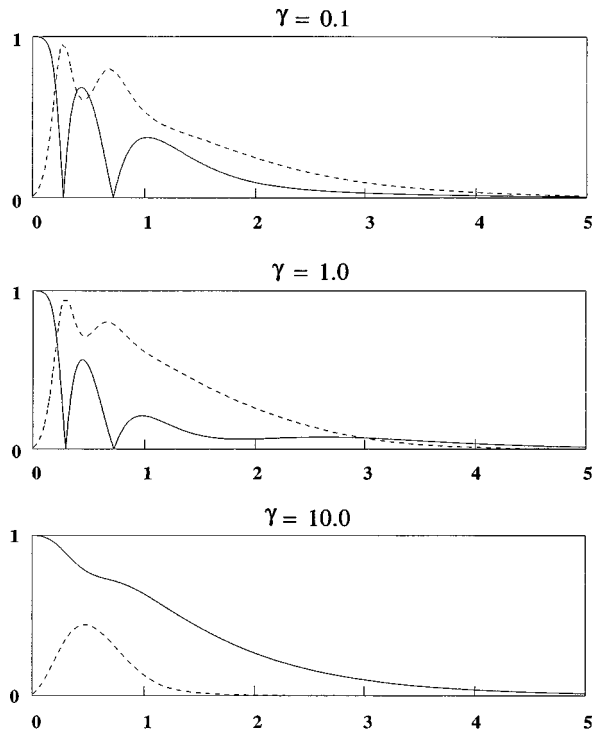


Fig. 1. Pump (solid curve) and Stokes (dashed curve) amplitudes as a function of time ( $\tau$ ) at a distance  $\chi = 50$ .

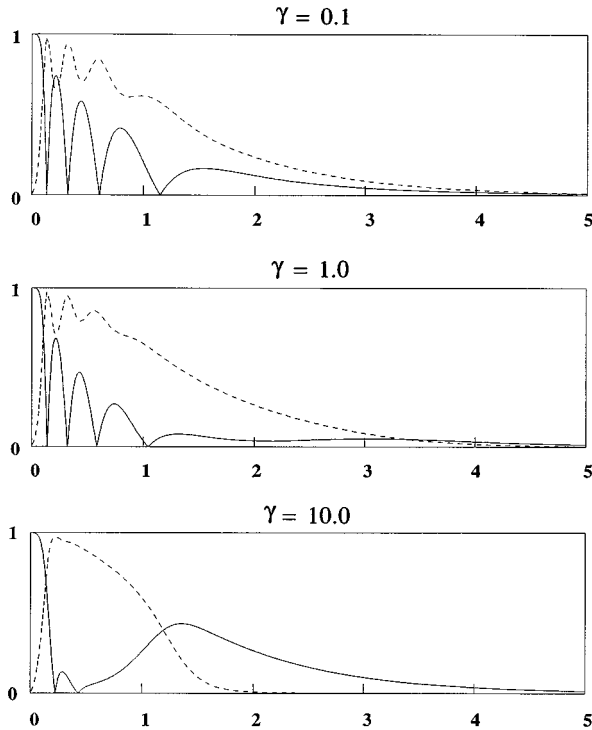


Fig. 2. Same as Fig. 1 but for  $\chi = 100$ .

ues because previous studies showed that accordions appear on this length scale in the transient regime.<sup>1,8</sup> The behavior as a function of time is nearly the same at all three values of  $\chi$  when  $\gamma = 0.1$  and  $\gamma = 1.0$ . The peaks of the pump oscillations appear at somewhat earlier times

when  $\gamma = 1.0$  than when  $\gamma = 0.1$ , and the size of the maxima is somewhat diminished, but the differences are not large. By contrast, the evolution when  $\gamma = 10.0$  is quite different. While accordionlike oscillations are visible at  $\chi = 100$  and  $\chi = 200$  when  $\tau < 1$ , the number of maxima is smaller than in the transient regime, and the maxima occur at earlier times. That is consistent with our theoretical expectation since true transient behavior is expected only when  $\gamma\tau \lesssim 1$ . In addition, a peak can be observed at  $\tau \approx 1.3$  when  $\chi = 100$  and at  $\tau \approx 1.8$  when  $\chi = 200$ ; this peak corresponds to the onset of stationary behavior. A similar but much smaller peak can be observed between  $\tau = 3$  and  $\tau = 4$  when  $\gamma = 1.0$ . To understand this peak's presence, we note that Eq. (3c) implies

$$X(\chi, \tau) = \int_{-\infty}^{\tau} A_1(\chi, \tau'') A_2^*(\chi, \tau'') \exp[-\gamma(\tau - \tau'')] d\tau'' \quad (6)$$

When  $\gamma$  is small, then  $X$  is affected by values of  $A_1$  and  $A_2$  in the neighborhood of  $\tau = 0$  even when  $\tau$  is large. Since the intensity near  $\tau = 0$  is large,  $X$  remains large when  $\tau$  is large. By contrast, when  $\gamma$  is large, the value of  $X$  at  $\tau$  is affected only by the values of  $A_1$  and  $A_2$  over times of the order of  $\gamma^{-1}$  before  $\tau$ , implying that, when  $\tau$  is large,  $X$  must be small, which, if we refer to Eqs. (3a) and (3b), implies in turn that the rate of pump depletion is slowed. Thus the peak appears.

In Figs. 4–6 we show the same data as in Figs. 1–3 after making the following transformation: We first recall that  $K^2(\tau) = |A_1(\chi, \tau)|^2 + |A_2(\chi, \tau)|^2$  and that  $K(\tau)$  is  $\chi$  independent. Letting  $T_\infty = \int_{-\infty}^{\infty} K^2(\tau) d\tau$ , we also define new time and space variables,

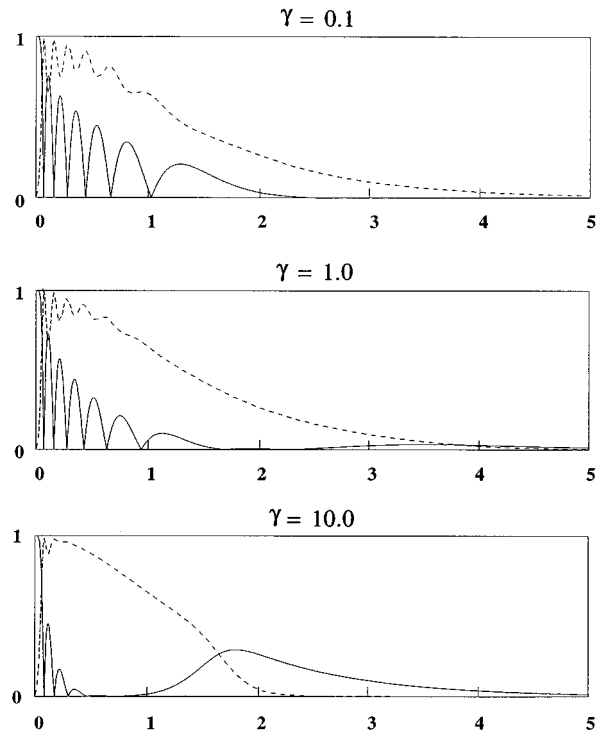


Fig. 3. Same as Fig. 1 but for  $\chi = 200$ .

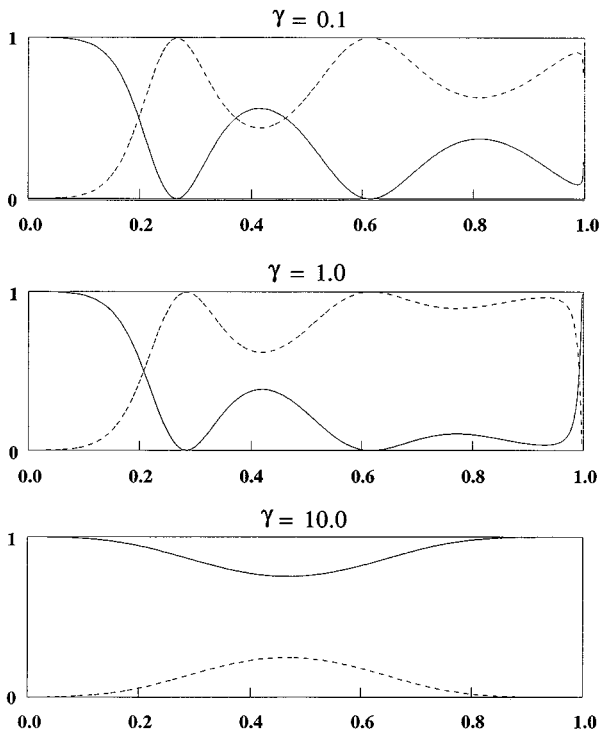


Fig. 4. Pump (solid curve) and Stokes (dashed curve) amplitudes, after transformation by Eqs. (7) and (8), as a function of time ( $\tau'$ ) at a distance  $\chi = 50$ . Note that the distance is  $\chi = 50$ , not  $\chi' = 50$ , to permit comparison with Fig. 1.

$$\tau' = \frac{1}{T_\infty} \int_0^\tau K^2(\tau'') d\tau'', \quad \chi' = T_\infty \chi, \quad (7)$$

and new dependent variables,

$$A'_1 = \frac{A_1}{K(\tau)}, \quad A'_2 = \frac{A_2}{K(\tau)}, \quad X' = \frac{X}{T_\infty}. \quad (8)$$

These transformations leave Eqs. (3) invariant except that  $\gamma \rightarrow \gamma T_\infty / K^2(\tau)$  so that, when  $\gamma = 0$ , this transformation is strictly invariant. It has previously been shown that, when  $\gamma = 0$ , this transformation transforms any set of initial conditions into a new, equivalent set in which  $K(\tau') = 1$  in the interval  $0 < \tau' < 1$  and  $K(\tau') = 0$  elsewhere. It is in these new variables that the self-similar nature of the accordions is most readily apparent. Referring to the case  $\gamma = 0.1$  in Figs. 4–6, we find that the behavior of the pump and the Stokes amplitudes as a function of  $\tau'$  at  $\chi = 50$  in the range  $0 < \tau' < 1$  is identical to the behavior of the pump and the Stokes amplitudes at  $\chi = 100$  in the range  $0 < \tau' < 0.5$  and is also identical to the behavior of the pump and the Stokes amplitudes at  $\chi = 200$  in the range  $0 < \tau' < 0.25$ . This behavior in which the pump and the Stokes oscillations are squeezed from the right as the pump and the Stokes waves evolve in  $\chi$  is the reason that these solutions are referred to as accordions. We note, however, that the pump amplitude has a sharp rise to  $A'_1 = 1$  at  $\tau' = 1$ . The reason for this sharp rise is the onset of stationary behavior. The behavior at  $\gamma = 1.0$  is similar to that at  $\gamma = 0.1$ , but the rise of the pump amplitude at  $\tau' = 1$  is more visible. While the behavior at  $\gamma = 10.0$  is quite dif-

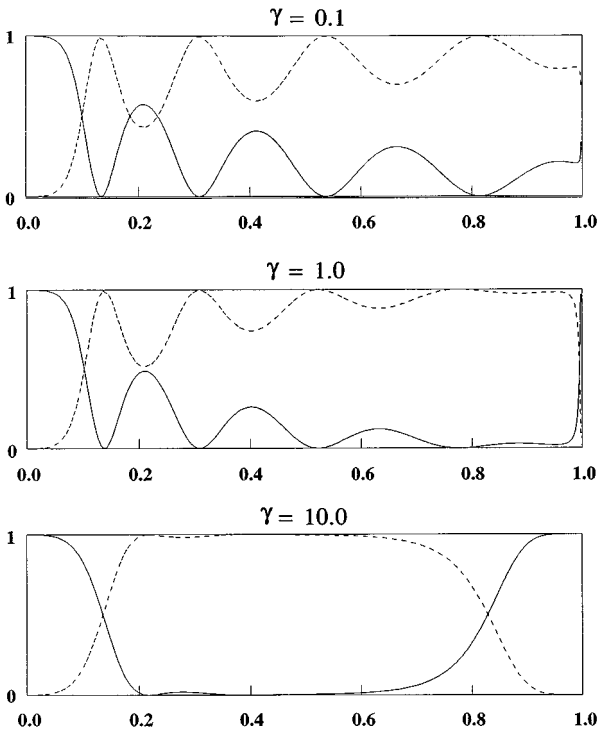


Fig. 5. Same as Fig. 4 but for  $\chi = 100$ . Note that the distance is  $\chi = 100$ , not  $\chi' = 100$ , to permit comparison with Fig. 2.

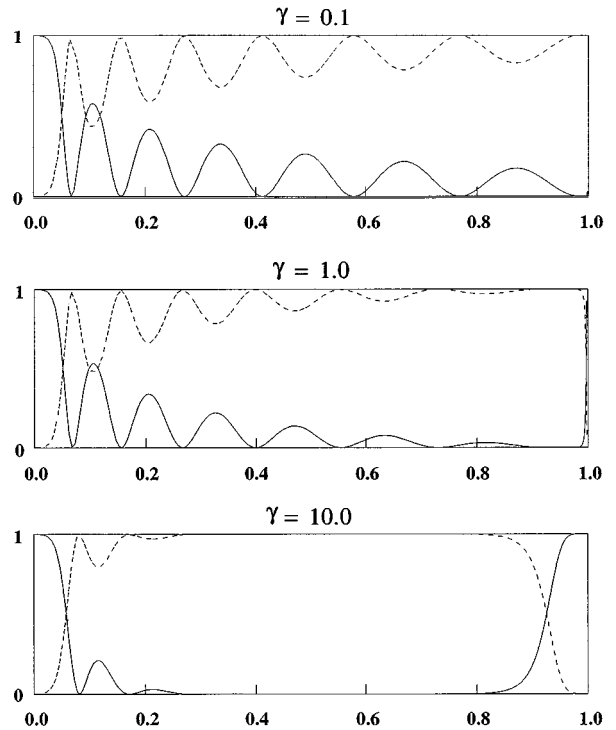


Fig. 6. Same as Fig. 4 but for  $\chi = 200$ . Note that the distance is  $\chi = 200$ , not  $\chi' = 200$ , to permit comparison with Fig. 3.

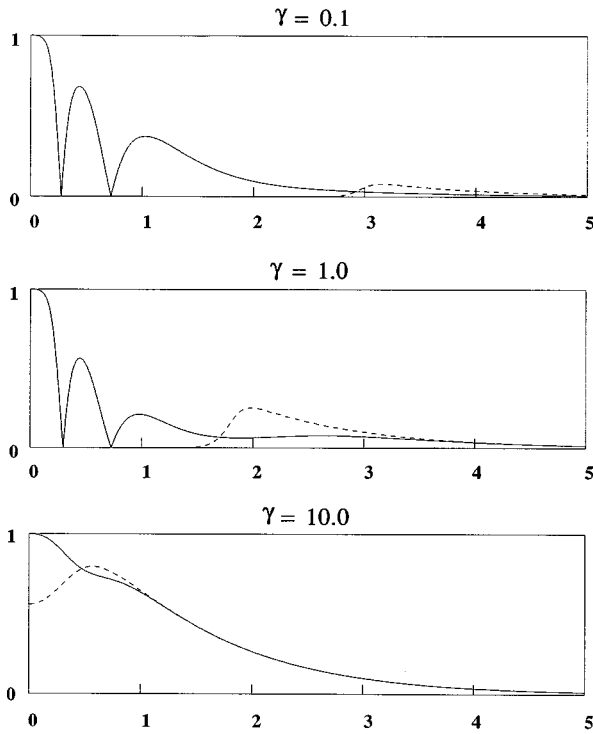


Fig. 7. Pump amplitude (solid curve) as a function of time ( $\tau$ ), compared with the prediction of the stationary-regime theory (dashed curve) at a distance  $\chi = 50$ .

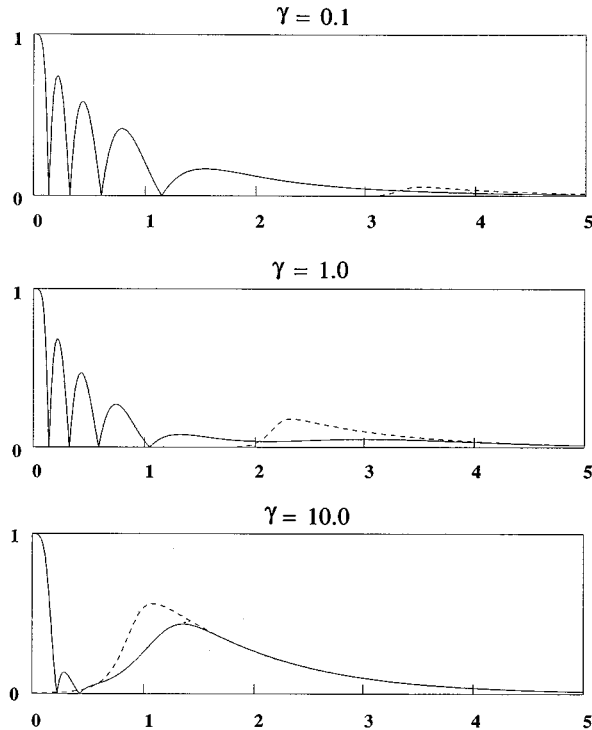


Fig. 8. Same as Fig. 7 but for  $\chi = 100$ .

ferent, and the rise of  $A_1'$  is quite visible near  $\tau' = 1$ , accordionlike oscillations are clearly visible near  $\tau' = 0$  when  $\chi = 200$ .

In order to determine precisely when the onset of the stationary regime occurs, we compare the pump ampli-

tude with the predictions of Eqs. (4) in Figs. 7–9. The predictions of Eqs. (4) are never useful when  $\gamma = 0.1$ , which is not surprising since the behavior is not expected to be stationary until  $\gamma\tau \gg 1$ , i.e.,  $\tau \gg 10$ , and at this value of  $\tau$  the pump and the Stokes amplitudes are vanishingly small. In the case  $\gamma = 1.0$  the predictions of Eqs. (4) are nearly correct when  $\tau \geq 4.0$  at  $\chi = 50$ , when  $\tau \geq 4.5$  at  $\chi = 100$ , and when  $\tau \geq 5.0$  at  $\chi = 200$ . In the case  $\gamma = 10.0$  the predictions of Eqs. (4) are nearly correct when  $\tau \geq 1.2$  at  $\chi = 50$ , when  $\tau \geq 1.6$  at  $\chi = 100$ , and when  $\tau \geq 2.0$  at  $\chi = 200$ . When  $\chi = 200$ , we find in both cases that accordionlike behavior is visible at early times, followed by a region in which the pump amplitude rises and eventually becomes equal to the predicted values of the stationary theory. This point increases as  $\chi$  increases.

It is natural to search for a new transformation that would generalize Eqs. (7) and (8) in the case of nonzero  $\gamma$ . This question has been examined by Levi *et al.*,<sup>10</sup> who found such a transformation in the case of nonzero  $\gamma$  but who also found that this transformation only applies for a particular exponential form for the pump and the Stokes amplitudes. This form is not useful to us because it corresponds to pump and Stokes waves with infinite energy. We empirically examined a variety of variable transformations, including that suggested by Levi *et al.*,<sup>10</sup> without finding one that was consistent with all our data.

In this report we have studied the transition between transient and stationary behavior in stimulated Raman scattering. We have found that, when  $\gamma \leq 1$ , the behavior is essentially transient, and, even when  $\gamma = 1$ , the behavior is nearly what is predicted by the transient theory, although there is some displacement of the pump maxima to earlier times and a decrease in their magnitude. At

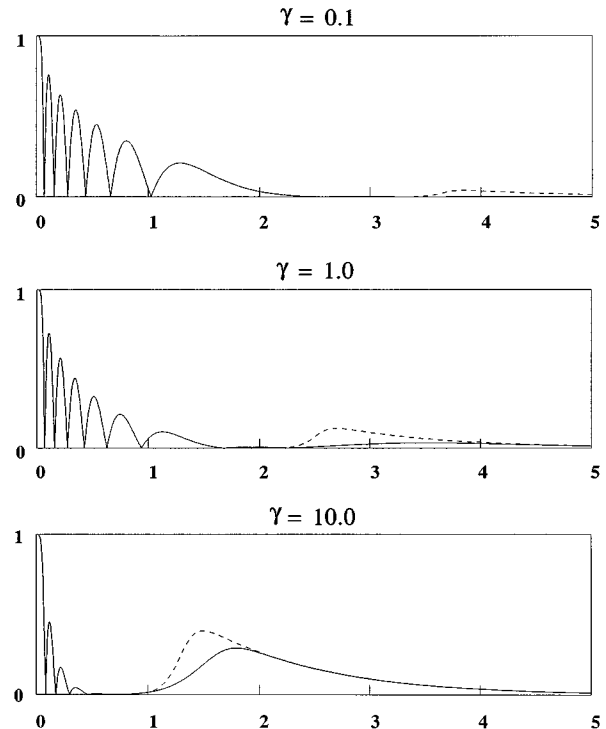


Fig. 9. Same as Fig. 7 but for  $\chi = 200$ .

large times there is also a transition to stationary behavior. Even when  $\gamma = 10$ , accordionlike oscillations can be observed when  $\tau \lesssim 1$  and  $\chi \gtrsim 100$ . These results bode well for the experimental proposal of Wessel *et al.*<sup>2</sup> to study accordions by use of the early times in a long-duration pulse.

### ACKNOWLEDGMENT

The work of C. R. Menyuk was supported by the Advanced Research Projects Agency through the U.S. Air Force Office of Scientific Research.

### REFERENCES AND NOTES

1. For a historical review that emphasizes self-similarity, see C. R. Menyuk, "Self-similarity in stimulated Raman scattering: an overview," in *Self-Similarity in Stimulated Raman Scattering*, D. Levi, C. R. Menyuk, and P. Winternitz, eds. (Les Publications CRM, Montreal, 1994), pp. 1–27.
2. J. G. Wessel, P. R. Battle, and J. L. Carlsten, "Stimulated Raman scattering in a multi-pass cell," in *Self-Similarity in Stimulated Raman Scattering*, D. Levi, C. R. Menyuk, and P. Winternitz, eds. (Les Publications CRM, Montreal, 1994), pp. 125–148.
3. M. D. Duncan, R. Mahon, L. L. Tankersley, G. Calame, G. Hilfer, and J. Reintjes, "Transient stimulated Raman scattering," in *Self-Similarity in Stimulated Raman Scattering*, D. Levi, C. R. Menyuk, and P. Winternitz, eds. (Les Publications CRM, Montreal, 1994), pp. 149–172.
4. D. C. MacPherson, R. C. Swanson, and J. L. Carlsten, "Stimulated Raman scattering in the visible with a multi-pass cell," *IEEE J. Quantum Electron.* **25**, 1741–1746 (1989).
5. M. D. Duncan, R. Mahon, L. L. Tankersley, and J. Reintjes, "Transient stimulated Raman amplification in hydrogen," *J. Opt. Soc. Am. B* **5**, 37–52 (1988).
6. C.-S. Wang, "Theory of stimulated Raman scattering," *Phys. Rev.* **182**, 482–494 (1969).
7. C. R. Menyuk and T. I. Seidman, "Transient stimulated Raman scattering," *SIAM J. Math. Anal.* **23**, 346–363 (1992).
8. C. R. Menyuk, D. Levi, and P. Winternitz, "Self-similarity in transient stimulated Raman scattering," *Phys. Rev. Lett.* **69**, 3048–3051 (1992); C. R. Menyuk, "Long-distance evolution in transient stimulated Raman scattering," *Phys. Rev. A* **47**, 2235–2248 (1993).
9. G. Hilfer and C. R. Menyuk, "Stimulated Raman scattering in the transient limit," *J. Opt. Soc. Am. B* **7**, 739–749 (1990).
10. D. Levi, C. R. Menyuk, and P. Winternitz, "Similarity reduction and perturbation solution of the stimulated-Raman-scattering equations in the presence of dissipation," *Phys. Rev. A* **49**, 2844–2852 (1994).